# Characterization of Horizontally Grown Silicon Nanowires in Aluminum Thin Films

Khaleel N. Abushgair [a,*], Husam H. Abu-Safe [b], Hameed A. Naseem [b], Mahmoud A. EL-Sabagh [b], Brian L. Rowoen [b], Avnish K. Srivastava [c], Samir M. El-Ghazaly [b]

*[a]Department of Mechanical Engineering, Al-balqa Applied University, Amman, Jordan*

*[b]Department of Electrical Engineering, University of Arkansas, Fayetteville, AR, 72701, U.S.A*

*[c]National Physical Laboratory, New Delhi, India*

## Abstract

Characterization of silicon nanowires grown horizontally through aluminum thin films was conducted. We show in our work that the fabrication process of these wires depends mainly on the thermally-activated silicon diffusion in-between the boundaries of aluminum grains. The diffusion of silicon through grain boundary is much lower than the grain bulk. Therefore, silicon starts to accumulate and form a wire shape structure along these grain boundaries. At 600 C, these accumulations form a continuous network of nanowires. The results are unique in the fact that these nanowires are pushed to grow horizontally instead of the more common vertical direction. The majority of obtained nanowires have a diameter of 75 nm and a length > 5 μm.

## 1. Introduction

The continued scaling of silicon-based integrated circuit (IC) technology has produced need for a new generation of devices. Silicon nanowires (SiNWs) have proved to be valuable as research devices and as building blocks for nanotechnology [1]; this is proved by the recent progress of transistors and lasers built with nanowires [2]. However, fabrication of large amount of nanowires especially in an isolated form is still under research.

Self assembly of nanostructures provide a reasonably cost efficient and easy to implement way to fabricate nanoelectronic components [3, 4]. Many different attempts to fabricate silicon nanowires have been devised, including the vapor liquid solid method (VLS) [5] and the solid liquid solid method (SLS) [6] with metal catalysts, and laser ablation of powder silicon [7]. However, the fabricated nanowires using these methods are still in need to be incorporated into devices and to be tested as charge or signal carriers. There have been recent studies [8, 9] that report methods to fabricate aluminum-silicon nanowire networks. The method reported in reference 8 produced wires that can actually conduct currents. The web-like network was fabricated by de-alloying an aluminum-silicon thin film through selective chemical etching. The current that propagated through the network depends, in general, on the etch time of the alloyed film. However, lack of control over the design of this network, reduces its appropriateness when well designed architecture is required.

In this paper, we report a method similar to the one reported in reference 9 to grow horizontal network of silicon nanowires on silicon substrate. We also show that this method is similar to the SLS method but yet different in the temperature where this process takes place and also in using aluminum as a catalyst instead of gold or nickel commonly used in this process . Furthermore, we show that the use of aluminum as a catalyst results in a network of nanowires that grows in the horizontal direction rather than the vertical direction. Effect of the annealing temperature on the nanowire network is investigated and a possible growth mechanism is presented.

## 2. Experimental Parameters

In all our reported experiments, the used substrates were 5" silicon (100) wafers and 1"×1" Corning 7059 glass. Two sets of silicon samples were prepared. In the first set, the samples were cleaned with Acetone and the native oxide was removed by dipping the samples in a HF solution with 10% concentration for 2 minutes and then dried with filtered and compressed Nitrogen. In the second set a 300 nm of silicon oxide was thermally grown on the

silicon surface. In this oxidation process, the samples were placed inside a furnace with 3L/min oxygen flow at 950°C for 30 minutes. The oxide was patterned into various rectangular and circular shapes ranging in length from 12 μm to 200 μm. In one scheme the oxide was removed from the surface except those patterned regions (positive patterning). In the second scheme the oxide layer was removed only from the regions corresponding to those in the previous scheme (negative patterning). This was done using the negative mask of the one in the first scheme. The glass samples were cleaned with acetone and dried in a nitrogen flow. A thin layer of aluminum (40 nm) was thermally evaporated (using Edwards Auto 306 vacuum coater) on all silicon wafers and the glass samples. The prepared samples where then cut into 1 cm× 1 cm pieces using a diamond cutting saw. The samples were placed into a quartz tube for annealing. The temperature controller was able to maintain the sample temperature up to accuracy of ±0.1°C. To minimize the film oxidation, Argon was introduced in the annealing tube at a flow rate of 94 sccm and the pressure inside the tube was maintained at 200 Torr. Annealing time was fixed to 2 hours and the temperature range varied from 500°C to 600°C. To observe the morphology of the silicon surface, the samples were dipped for 2 minutes in an aluminum etchant solution (85% phosphoric acid, 5% nitric acid, 5% acetic acid, and 5% DI water at 40°C) and then dried in a nitrogen flow.

The features of the samples' surface morphology were examined using scanning electron microscopy (SEM) and atomic force microscopy (AFM). The compositional analysis was done using energy dispersive X-ray spectroscopy (EDX) and the crystalline structure of the samples was analyzed using cross sectional transmission electron microscopy (XTEM).

## 3. Results and Discussion

The overall results for the samples without the oxide layer are shown in SEM images of Figure 1. Figure 1a shows the calm and smooth texture of the film surface before annealing. After 2 hours of annealing at 600°C, dramatic changes in the surface morphology were observed. Figure1b shows the various confined structures on the silicon surface after this annealing. These structures can be divided into two main types with respect to their sizes. The smaller structures formed a web-like interconnected network that was observed all over the surface. Figure 2 shows 3D AFM image of these wires on the silicon surface. The wires making this network had an average diameter size of 75 nm. It is observed that these nanowires grow in a horizontal, rather than the more typical vertical direction. The individual nanowires seem to connect at various points to form this web. The lengths of these wires were comparable and reached few microns. The second type of structures is the larger island-like material clusters that also connect the individual wires and are part of the web structure. Figure1c shows the annealed samples after aluminum was removed. The nanowires web structure is still observed in these samples. However, the island structures seem to loss their cluster forms into a deformed crater shapes with hallow interior. When comparing these results to the ones obtained from the glass samples we found no structural formations created on the surface. Figure 3 shows the SEM image for the glass samples after annealing at 600°C for 2 hours. The major observation in these films was the cuts created in the film due to thermal coefficient mismatch between aluminum and glass ($\alpha_{aluminum}$=23 ×10$^{-6}$ K$^{-1}$, $\alpha_{glass}$=0.46 ×10$^{-6}$ K$^{-1}$).

To determine the elemental composition of the confined structures seen on the silicon samples before and after annealing, EDX spot measurements were taken at several locations on the surface of the various structures with an electron beam of 10 keV and spot size of 1.7 nm.

The EDX spectra of the samples before and after annealing are shown in Figure 4. Figure 4a shows the spectral pattern of the samples before annealing indicating the topical presence of the aluminum film on the sample. The oxygen peak in the pattern is due to the aluminum oxide on the film. Figure 4b is the pattern of a spot on the wire before aluminum is removed indicating the silicon composition of these wires. Nonetheless, this peak could come from the silicon wafer underneath the film as a result of film cracking. But no cracks were observed in the films even with very high magnification. The absence of the aluminum peak from this pattern suggests a unitary composition of these wire structures. The important concept from this is the idea that the silicon material can be confined to a nanosize diameter, micron-long, horizontal structures in the aluminum film. The confining locations had to be the grain boundaries of the metal film. The small oxygen peak in the pattern comes from the remaining aluminum oxide atop the wire. Figure 4c shows the elemental composites of the surface outside the wire and away from the island regions. These spot measurements were made before aluminum removal. The comparable aluminum and silicon peaks in this case indicate the thinning of the aluminum layer on these locations. This thinning behavior could come from the aluminum expansion, where stretching the film during annealing lead to the reduction of film thickness. However, this reduction is not sever and the surface is still going to be covered with an aluminum layer that shows a strong signal. Figure 4d is the EDX pattern coming from the islands on the surface; these formations are made mainly from aluminum as can be seen from the strong aluminum peak. However, the presence of the small silicon peak suggests a binary material composition existing as a result of silicon/aluminum alloying. Figure 4e is the EDX pattern coming from the annealed sample after aluminum was removed. This peak is representative of all confined structures indicating the dominant silicon composition in them.

Fabrication of SiNWs with catalysts has been described by other studies [10, 11]. In the VLS method the source for the vertically grown SiNWs is in the gas phase. In our samples, on the other hand, the source of silicon is the substrate itself, since there is no silicon in the ambient gas during annealing. While the SLS growth mechanism can be used as a possible explanation to describe the growth of these nanowires, the vast differences in the features of nanowires grown (vertical versus horizontal), annealing time, and process temperatures (typical SLS growth require temperatures on the order of 1000°C) would demand a different explanation of the growth mechanism.
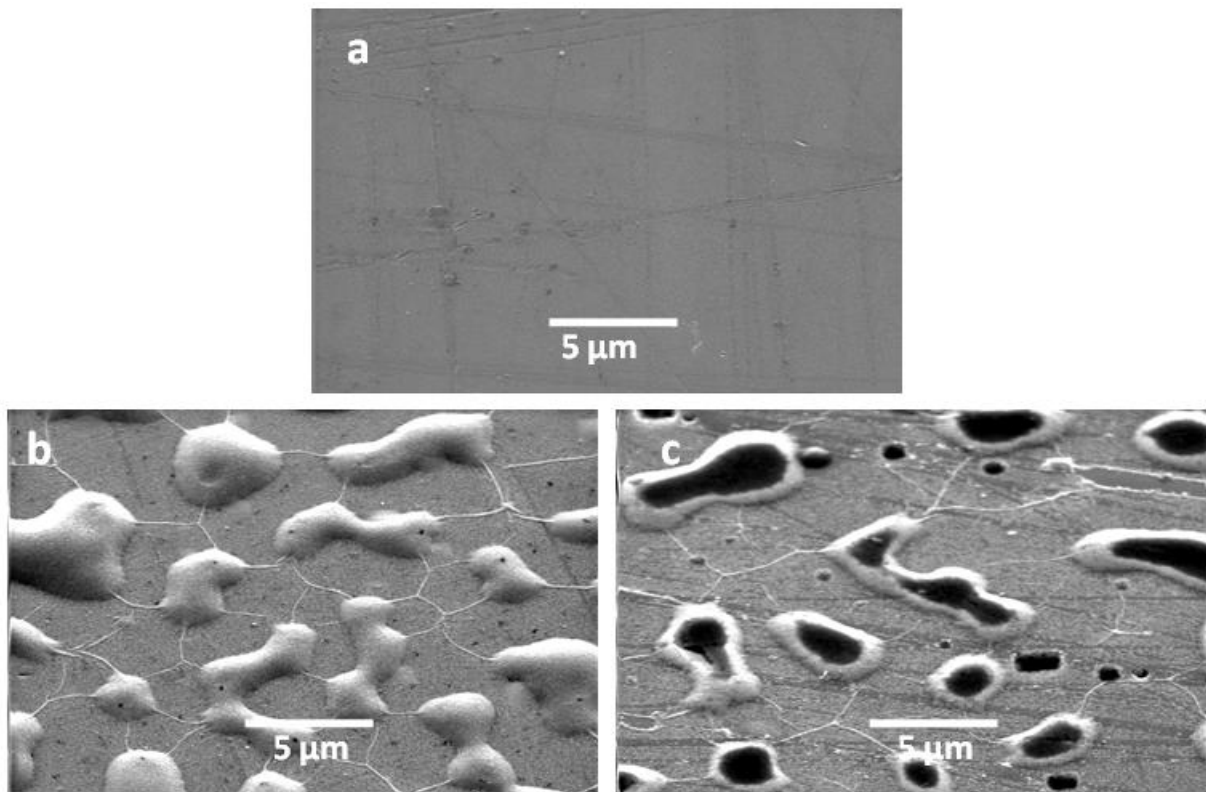
Figure 1. SEM image of the samples annealed at 600°C for 2 hours. The samples where tilted at 45° during imaging: a) SEM image of the sample before annealing, b) SEM image of the sample before aluminum was removed, c) SEM image of the sample after aluminum was removed. The black regions in c are where silicon had been etched at a faster rate.
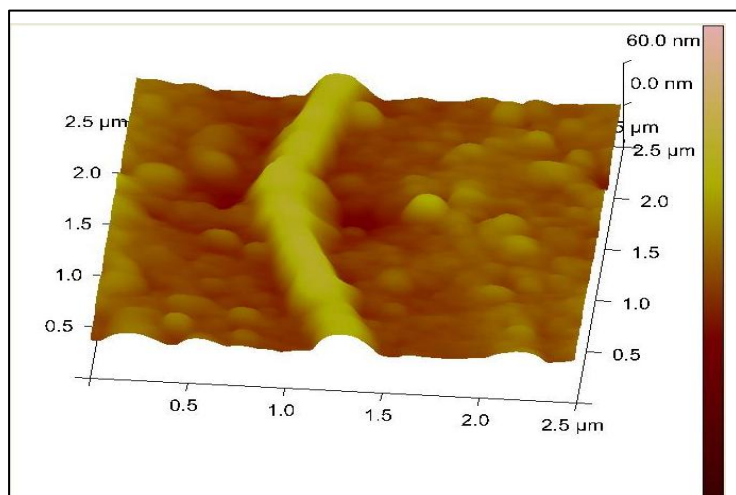


Figure 2. 3D AFM images of the samples annealed at 600°C for 2 hours after aluminum removal showing a wire formation created by the accumulations at the grain boundary.
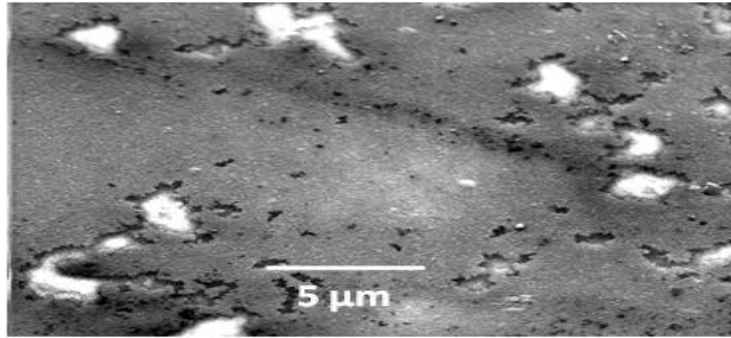
Figure 3. SEM of the glass sample after annealing at 600°C for 2 hours. The aluminum film did not show any confined structures on the film. The major observation is the cuts in the film due to thermal coefficient mismatch with the glass substrate.
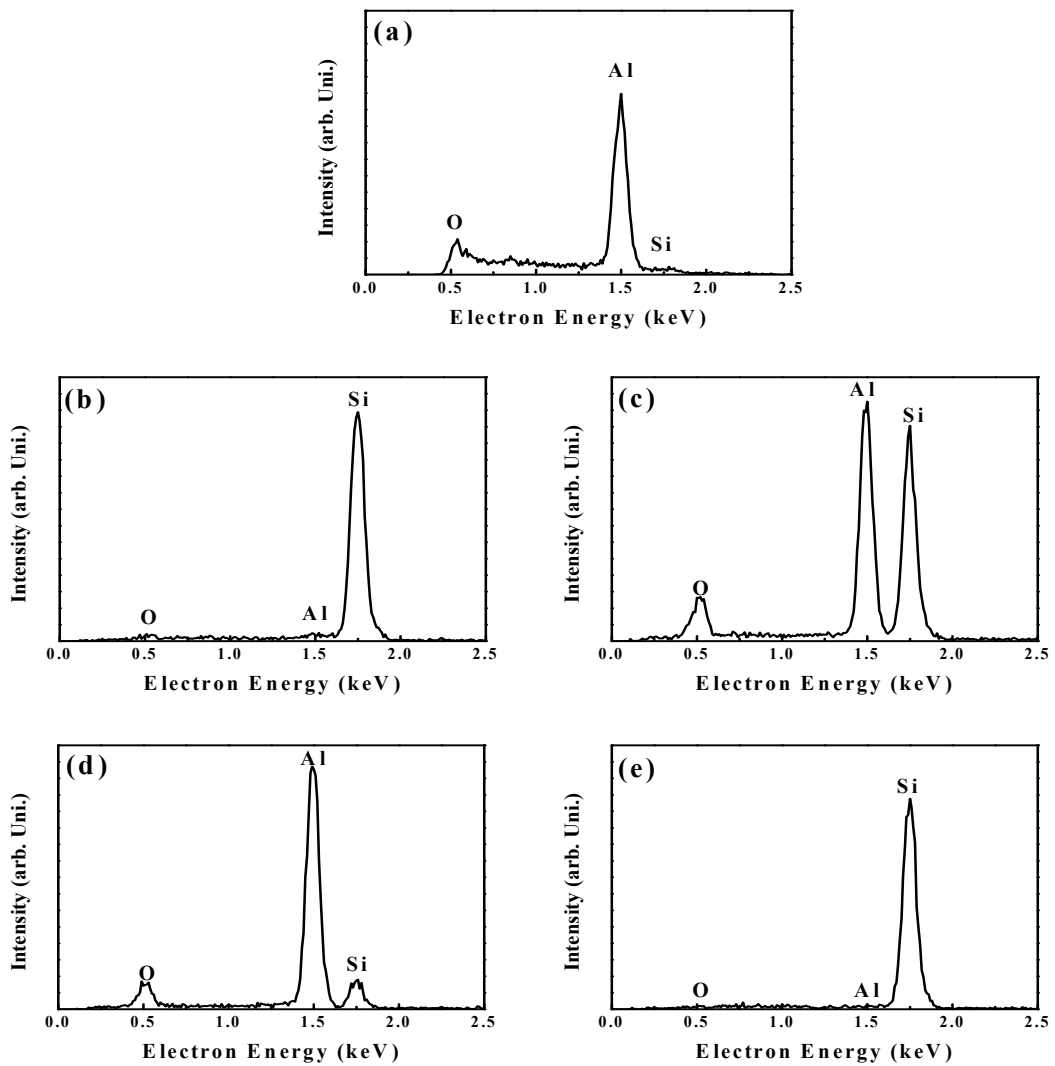


Figure 4. EDX spectrum pattern taken at a spot on the: a) aluminum surface before annealing, b) wire, c) off the wire, d) the island-like and d) surface after aluminum is removed.

To understand this mechanism, a temperature study of the silicon samples was conducted. Figure 5 shows the SEM images taken for the samples annealed at different temperatures for 2 hours. Starting with Figure 5a and the corresponding Figure 5a' which are the images of the silicon samples before and after removing the aluminum annealed at 500°C, respectively. In Figure 5a' (where aluminum is removed) the silicon surface appeared to have pitted regions indicating silicon etching during annealing. Also it is noted that the surface between the pitted regions is smooth which means that surface pitting occurred only at specific locations. These locations are where the silicon surface had defects that would increase the film internal stress locally. Mixing of silicon with aluminum on this location is provoked in this case. The etched silicon forms with the aluminum an alloy material where it fills the pitted region. From these alloy regions and as the silicon gradient concentration increases, silicon starts to diffuse through the aluminum film toward the grain boundaries in the film. However, the diffused amounts are not sufficient to reach the grain boundaries or even redeposit significantly on the silicon surface. Therefore, the etched silicon is washed off when aluminum removal process is performed. Figure 5b and the corresponding Figure 5b' are the SEM images at 550°C before and after aluminum removal, respectively.  The islands in these samples (shown in Figure 5b) are larger but yet they are not well defined. The pitted regions in Figure 5b' are larger than the pitting in the previous sample indicating more etching at this temperature.  Moreover, it is noted that a layer of silicon is deposited on the surface around the pitted regions. This second layer is not observed in the previous samples. However, the silicon surface between the pitted regions (partially shown in the image) is still smooth indicating the selective aluminum etching of the silicon surface.

Figure 5c and Figure 5c' shows the samples annealed at 580°C before and after aluminum is removed, respectively. On the sample with the aluminum film, a well-defined dark circular spots with a notch at its central region is shown.  The diameter of these spots had an average of 3μm. When examined by EDX, these regions showed a dominant aluminum composition (see Figure 6a). The signal outside these circular spots (Figure 6b) showed only a strong silicon peak. As we have mentioned before, during high temperature annealing, the layer thickness reduces to the extent that aluminum signal becomes very weak. Most of the aluminum film cluster where silicon is being etched rapidly. This makes the aluminum film wear off in between regions. Therefore, these dark regions mark the locations where the large clusters will form.

As annealing temperature ramps up, silicon starts to erupt and diffuse from the aluminum clusters into the film. The size of these clusters increase and eventually forms an island-like structure. Figure 5d and Figure 5d' are the images of the sample annealed at 590°C before and after aluminum removal, respectively. The shapes of these islands are determined and defined by the grain boundaries of the aluminum film. On the other hand, as the silicon diffuses away from the highly concentrated regions and because diffusion is confined through aluminum film it forms a lib structure around the pitted regions as shown in Figure 5d'. Depending on the film thickness, the silicon

will continue to diffuse until the film cannot hold any more silicon. Therefore, silicon deposition on the surface becomes imminent.  A continuous second layer as the one seen in this figure will form. Figure 7 is schematic presentation of the formation mechanism of the clustered regions in the film. The erupted silicon etch from the walls of the crystalline silicon surface leaving behind inverted pyramids showing the (100) nature of the wafers.

The EDX patterns for the island formations are shown in Figure 8. The composites of the islands at the center and the edges are shown in Figure 8a and Figure 8b, respectively. The islands are mainly made of aluminum and silicon structure which could be in the form on an alloy. Since the solubility of silicon in aluminum is limited to 12.6 wt% [12] and due to the high silicon gradient concentration in these regions, silicon continues to diffuse through the aluminum layer until it redeposit on the surface or at the ground boundary forming the anticipated SiNWs. Pitted regions as well a second layer are observed everywhere on the surface but with different sizes. The smaller pitted regions are what make the surface between the larger regions look rough.

Figure 9a shows a XTEM image of the samples annealed at 600°C after aluminum was removed. The formation of a second silicon layer is clear in this image. Most of deposited silicon grows epitaxialy on the surface [13]. However, since the diffusion is random, the new layer will contain microcrystalline or even amorphous phases.  The halos in the selected area diffraction (SAD) image shown in Figure 9b indicate the presence of these microcrystalline regions in the deposited layer.

Figure 10a and Figure 10b shows the SEM images of the positively patterned oxide (PPO) and negatively patterned oxide (NPO) of the silicon samples after aluminum was removed, respectively. During annealing, silicon and aluminum interacted only in the exposed regions where the oxide was absent. On the other hand, since silicon diffuses in aluminum films for long distances (typically 200 to 300 μm) [14], large accumulations of silicon were observed on top of the oxide layer. This can be seen in the NPO samples where most of the surface was covered with the oxide layer. The cuts in the oxide are the only openings from where silicon will diffuse. Therefore, the diffusion is faster and the silicon deposits further on top of the oxide. Moreover, since silicon diffusion through grain boundaries is much slower than the grain itself-due to grain boundary trapping-the main depositions near the openings is in the form of SiNWs. Figure 11a shows an SEM image of the NPO sample where 80μm×120μ rectangular cut was made in the oxide. Figure 11b is a higher magnification image of the dashed rectangular shown in Figure 11a. The SiNWs network is shown clearly without any island-like formations.  The wire growth pattern in this case resembles the grain boundaries of the aluminum film. The only diffusion through these films is in the lateral direction therefore silicon diffuses from the openings through the film and deposits at the grain boundary. The silicon that accumulates in the grain boundaries starts to diffuse again further in the film leaving behind the accumulations in the grain boundary in the form of SiNWs. Nonetheless, far from these openings, the diffused silicon amounts become very small. Therefore, silicon tends to cluster forming silicon patches seen on top of the oxide away from the cut.
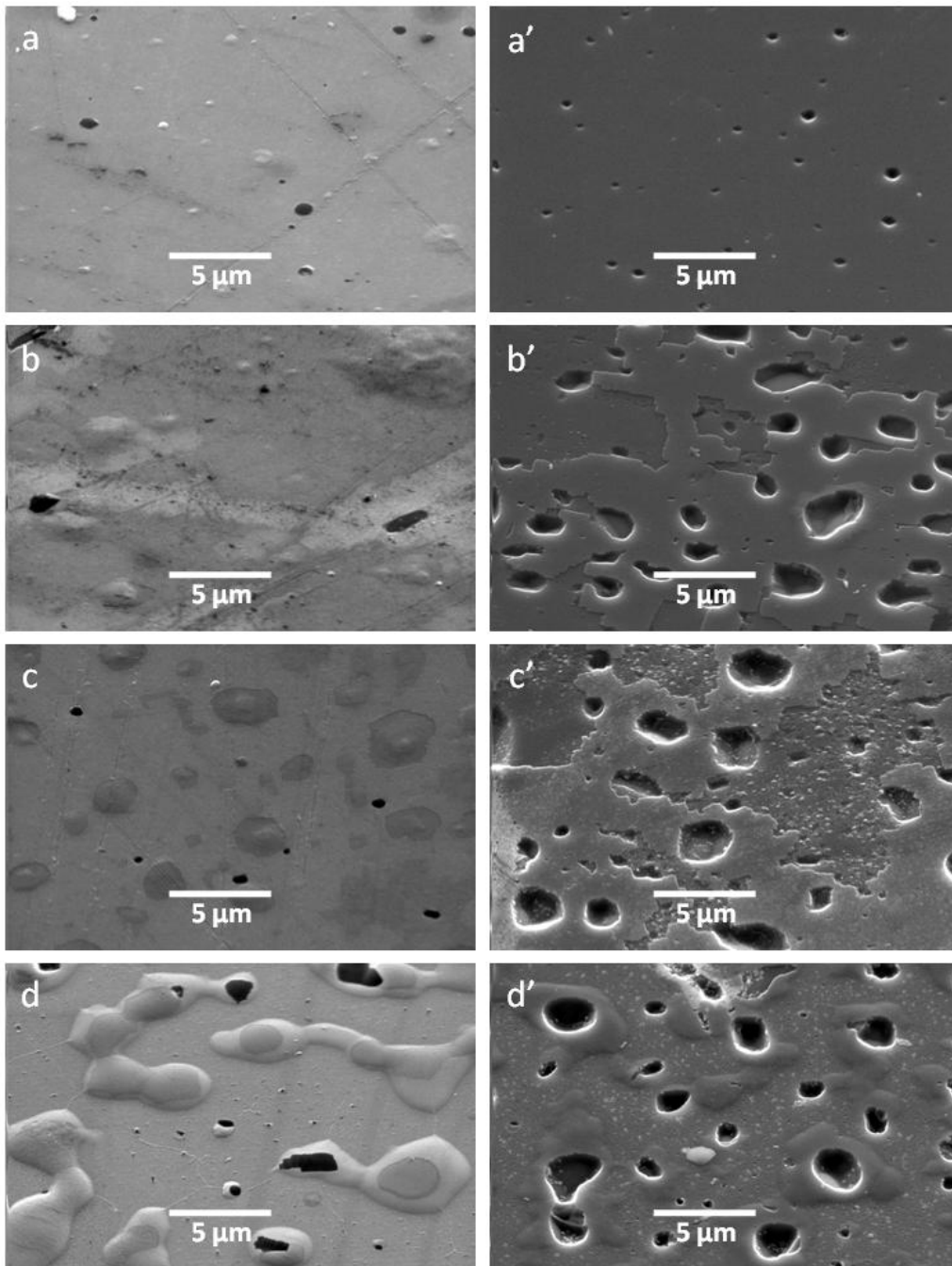
Figure 5. SEM images taken for the samples annealed for 2 hours at: a) 500°C, b) 550°C, c) 580°C, and d) 590°C. The primed letter indicate the image of the samples after aluminum was removed
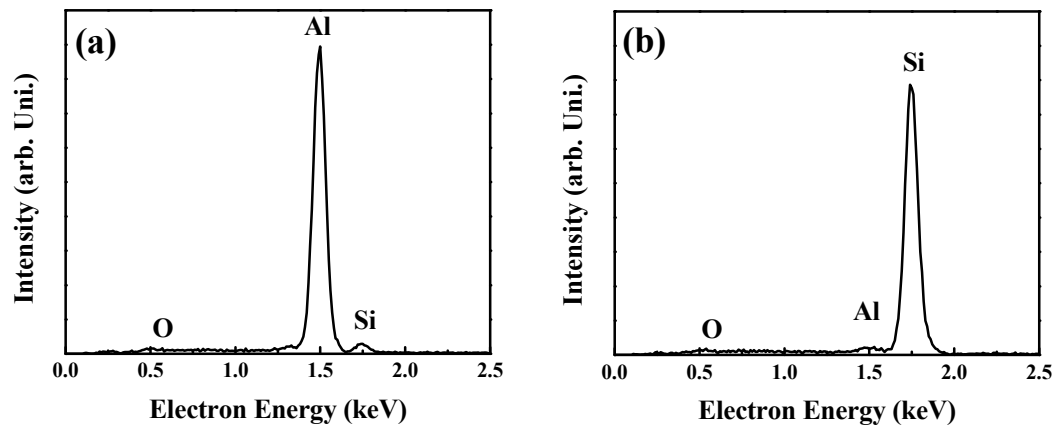
Figure 6. EDX pattern of the samples annealed a 580°C taken at: a) at the center of the dark circular region shown in Figure 5c and b) outside that circle.
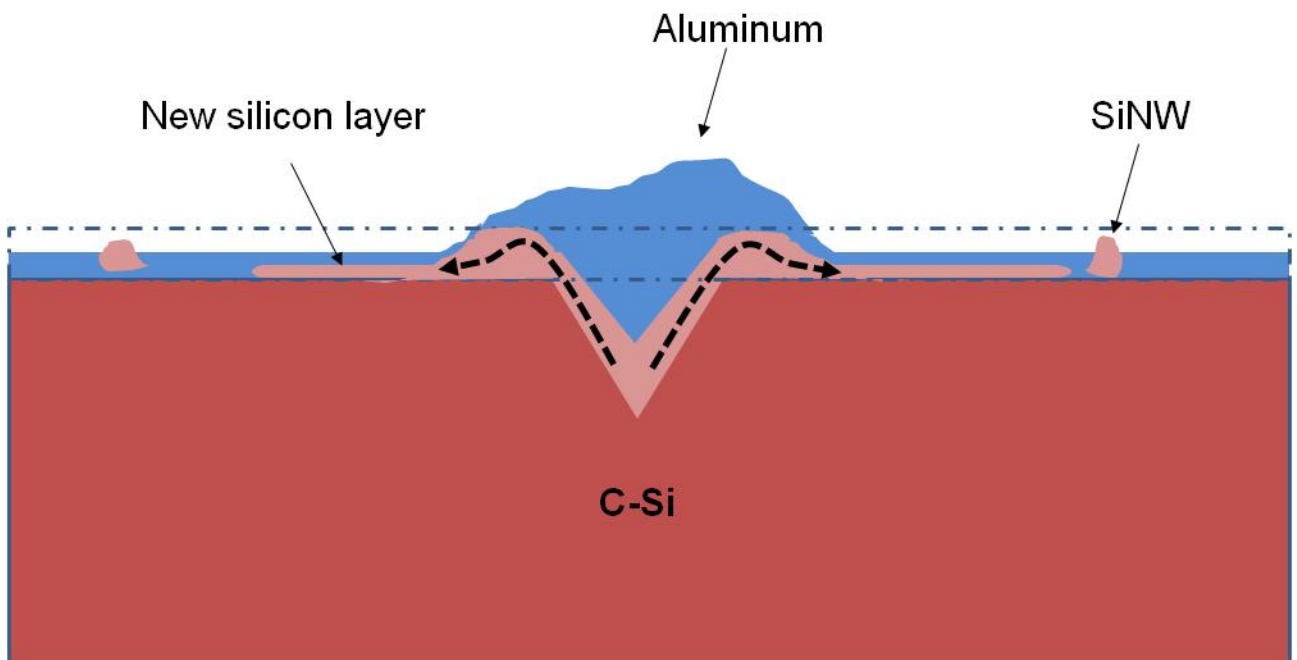


Figure 7. Schematic presentation of the material confined structures on the aluminum film. The dash dotted rectangle presents the thickness of the aluminum film before annealing.
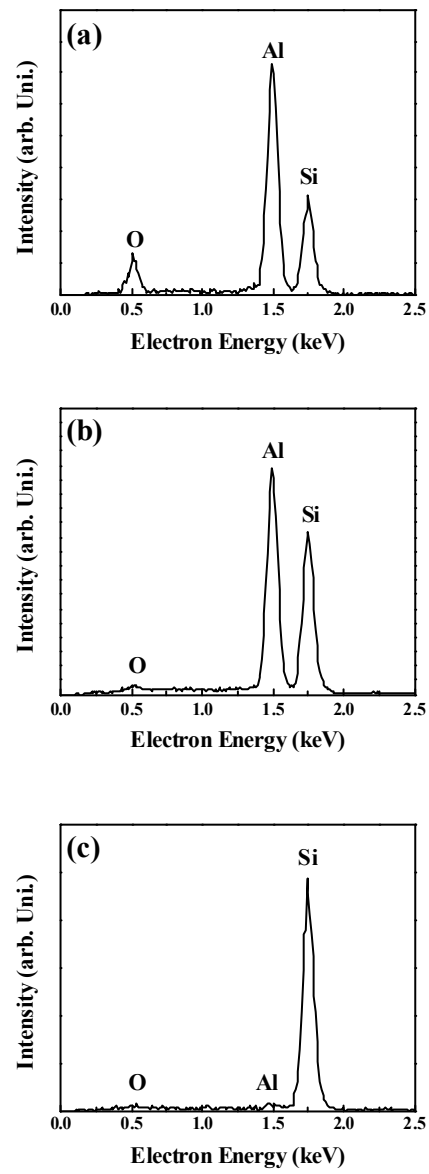
Figure 8. EDX pattern for the samples shown in Figure 5d. The spot measurements were taken at: a) the center of the circular spot, b) near the edge of the spot, c) on the silicon surface.
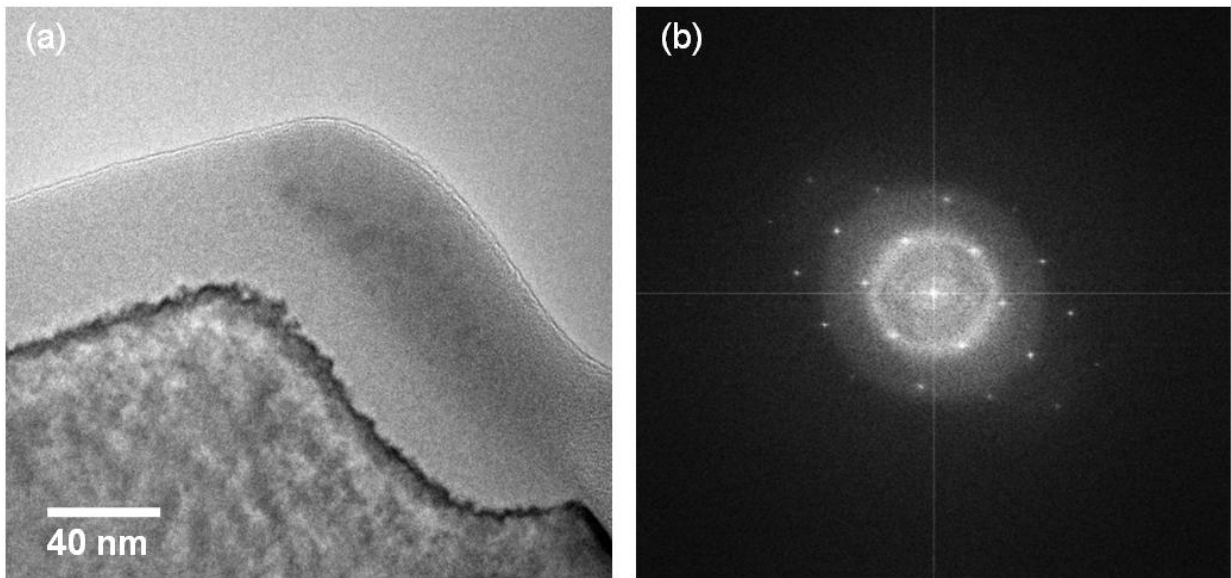
Figure 9. a) XTEM images of the samples annealed at 600°C for 2 hours after aluminum is removed. The image shows clearly the formation of a new layer on top of the silicon surface. b) SAD of the sample. The halos in the indicated a polycrystalline or even amorphous nature in this layer.
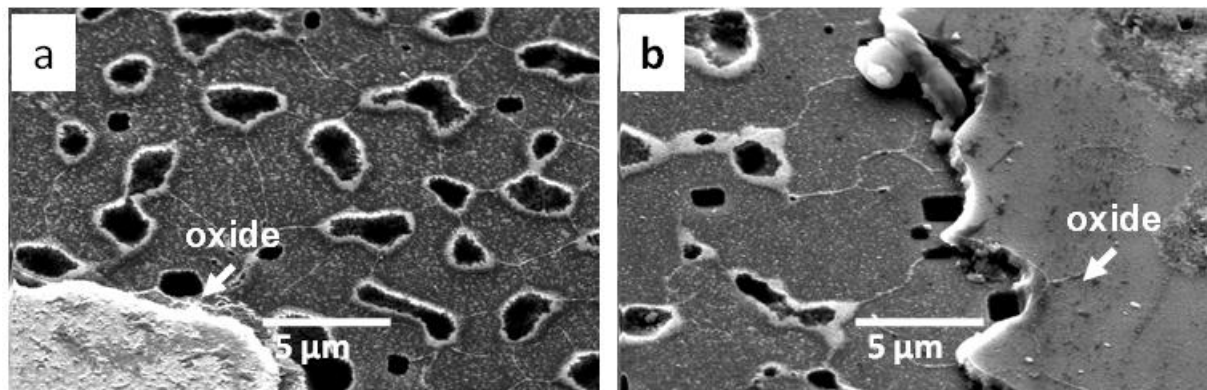


Figure 10. After aluminum removal, the silicon patches creating near the opening cuts in the oxide are removed also. The SEM images here are for a) PPO silicon samples and b) NPO silicon samples.
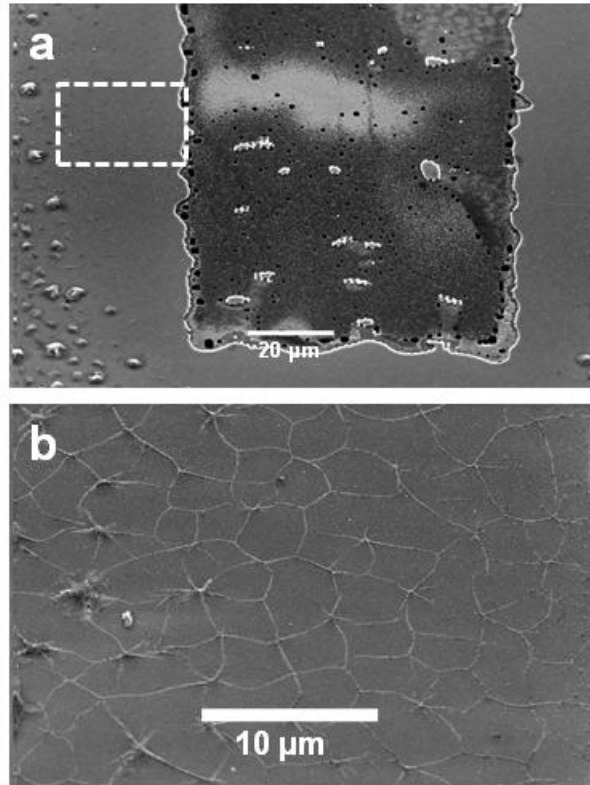
Figure 11. The opening cuts in the oxide acts as silicon source from where silicon will start to diffuser through the film. Near the cut most of the confined structures are in the form of SiNWs. The SEM images shown here for a) general overview and b) high magnification of the region indicated by the dashed rectangle shown in a.

The oxide covered surface is much less in the PPO samples. Therefore, the silicon does not have a preferred region to deposit. Silicon patch formation was observed near and away from the oxide edge. Small SiNWs were also observed on the oxide near the edge. Figure 12a and Figure 12b are the SEM images of the PPO before and after aluminum removal. The patches on the oxide seen near the cut before aluminum removal are the accumulated silicon and aluminum during annealing. When the aluminum was removed it took away the silicon parches leaving plane surface with no confined structures. The confided island-like and SiNWs are seen in the opened regions with no oxide where silicon and aluminum interacted in the same manner as the samples without the patterned oxide.
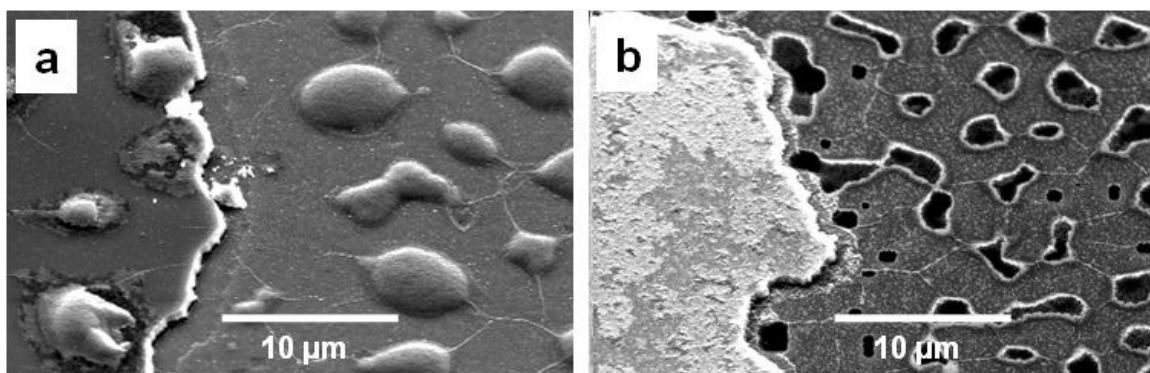


Figure 12. SEM images of the PPO silicon samples, a) before aluminum removal b) after aluminum removal. Small number of SiNWs were created near the edges of the oxide cuts since silicon had no preferred direction of diffusion.

## 4. Conclusion

In this experimental study, a horizontal network of SiNWs was grown on silicon substrate using aluminum as a platform for the growth process. The wires were grown at the grain boundaries of the aluminum film. The individual nanowires have lengths of few microns and a diameter of about 75 nm. As the silicon accumulates at these boundaries, it forms an interconnected web-like structure of SiNW. A comprehensive explanation of growth mechanism was presented in terms of silicon diffusion through aluminum and its subsequent deposition along the grain boundaries of the aluminum film.

## Acknowledgements

## References

[1] G.Timp, Nanotechnology, (Springer, New York 1999)

[2] Y. Wu, Y. Cui, L. Huynh, C. J. Barrelet, D. C. Bell, C. M. Lieber," Controlled Growth and Structures of Molecular-Scale Silicon Nanowires**,** Nano Letters Vol. 4, 2004, 433436

[3] X. Duan, Y. Huang, Y. Cui, J. Wang, and C. M. Lieber, "Indium Phosphide Nanowires as Building Blocks for Nanoscale Electronic and Optoelectronic Devices", Nature, Vol. 409, 2001,66-73

[4] W. U. Huynh, J. J. Dittmer, A. P. Alivisatos," Hybrid Nanorod-Polymer Solar Cells" ,Science, Vol. 295, 2002 ,2425-2427

[5] K.K. Lew, C. Reuther, A.H. Carim, J.M. Redwing," Template-directed vapor-liquid-solid growth of silicon nanowires" J. vac. Sci. technology. B, Vol. 20, 2002, 389-342

[6] .J. Xing , D.P. Yu, Z.H. Xi, Z.Q. Xue," Controlled growth of nanowires using annealing and pulsed laser.". Appl. Phys. A, Vol. 76, 2003, 551-556

[7] X . Chen, Y. Xing, J. Xu, J.Xiang, D. Yu," Metal-Induced Nickel Silicide Nanowire Growth Mechanism**.**",Chem. Phys. Lett., Vol. 374, 2003 ,626-630

[8] K. Jang, S. Hwang, and Y. Joo," Effect of capping layer on hillock formation in thin Al films",Metals and Materials International, Vol. 14, 2008 ,147-151

[9] V. H. Liu, H. H. Abu-Safe, H. A. Naseem, and W. D. Brown," Fabrication of Silicon Nanowire Network in Aluminum Thin Films" Mat. Res. Soc. Proc., Vol. 862, 2005. 363-368

[10] M. Paulose, C. A. Grimes, O. K. Varghese and E. C. Dickey, "Self-assembled fabrication of aluminum–silicon nanowire networks", Appl. Phys. Lett., vol. 81, 2002 ,153-155

[11] N. Ozaki, Y. Ohno, and S. Takeda, " Silicon nanowhiskers grown on a hydrogen-terminated silicon {111} surface",Appl. Phys. Lett., Voll.. 72, 1998, 3700-3702

[12] T. B. Massalski Binary Alloy Phase Diagrams (Materials Park, OH: ASM International) 1990

[13] K. Sharif, H. H. Abu-Safe, H. A. Naseem, W. D. Brown, M. Al-Jassim, R. Kishore, " Epitaxial Silicon Thin Films by Low Temperature Aluminum Induced Crystallization of Amorphous Silicon",Mat. Res. Soc. Proc., Vol. 910, 2007, 517-521

[14] J. O. McCaldin and H. Sankur, Diffusivity and Solubility of Si in the Al Metallization of Integrated Circuits Appl. Phys. Lett. , Vol.19, 1971, 524-527